THE JOURNAL OF PHYSICAL CHEMISTRY A

 VOLUME 107, NUMBER 12, MARCH 27, 2003

ARTICLES

Comparative Studies on Energy Relaxation Dynamics of Directly Linked Zn^{II} Porphyrin Dimers with Different Dihedral Angles

Hyun Sun Cho, Jae Kyu Song, Jeong-Hyon Ha, Sung Cho, and Dongho Kim*,†

Center for Ultrafast Optical Characteristics Control and Department of Chemistry, Yonsei University, Seoul 120-749, Korea

Naoya Yoshida and Atsuhiro Osuka*

Department of Chemistry, Graduate School of Science, Kyoto University, and Core Research for Evolutional Science and Technology (CREST) of Japan Science and Technology Corporation (JST), Kyoto 606-8502, Japan

Received: November 25, 2002

Photophysical properties of the strapped Zn^{II} porphyrin dimers (**S*n***, the strap chain between the porphyrins changes; $-O-(CH_2)_n-O-$, ***n*** = 1, 2, 3, 4, 8, and 10) and directly linked Zn^{II} porphyrin dimer (**Z2**) have been investigated by the steady-state and time-resolved spectroscopic methods. The reduced dihedral angle in **S*n*** gives rise to additional absorption bands around 400 nm as well as broad fluorescence in the near-infrared region. The fluorescence lifetimes of **S*n*** become gradually, but not so significantly, shorter as the strap length becomes shorter, indicating that the lifetimes of the lowest excited singlet states of **S*n*** are not affected much despite their structural distortions such as mean plane deviations and the existence of two conformers. Fluorescence excitation and viscosity-dependent fluorescence spectra suggest that **S2** exists as two conformers, A and B conformer, which has been also confirmed by X-ray data. The B conformer with a shorter interporphyrin distance has stronger interporphyrin interactions than the A conformer, which was revealed by the fluorescence excitation and fluorescence spectra. The A conformer is responsible for the shorter wavelength fluorescence at ca. 660 nm, whereas the B conformer gives rise to the near-infrared fluorescence. The photoinduced near-infrared absorption band was suggested to be characteristic of **S2**, which was not observed in **Z2**. The conformational dynamics of **S2** with a time constant of 15 ps was observed in the transient absorption and fluorescence upconversion measurements. From the comparative studies of **Z2** and **S*n***, we have demonstrated that the orientation of the two porphyrin macrocycles has a considerable effect on their photophysical properties.

1. Introduction

Light harvesting arrays in photosynthetic systems consist of aggregates of chlorophyll pigments with a unique rigid geometry maintained by the environmental protein.[1] There have been many studies to reveal the structure−property relationship regarding the nature of the intermolecular energy transfer and electronic delocalization in photosynthetic system.[2] At the same time, there have been a variety of trials to mimic the photosynthetic system for the possible applications as optical switch,

* To whom all the correspondences should be addressed.
† E-mail: dongho@yonsei.ac.kr. Fax: +82-2-2123-2434.

10.1021/jp022480h CCC: $25.00
Published on Web 02/27/2003

sensor, and solar cell.[3] Instead of chlorophylls, artificial porphyrin supramolecules have been prepared and investigated extensively because porphyrins are much easier to deal with due to their high thermal and chemical stability. The interporphyrin distance and relative orientation in the porphyrin arrays could be controlled effectively with a variety of linkers. Until now, most porphyrin arrays were linked by π-conjugated bridges between the adjacent porphyrin macrocycles because they give rise to the modifications of photophysical properties in a satisfactory manner.[4−10] The excitonic[11] and cumulenic (π-electron delocalization)[4] resonance interactions were considered to explain these changes as well as the effect of the bridges between the two porphyrin moieties. The energy relaxation dynamics of the porphyrin arrays were also observed to change drastically as a function of the number of porphyrin units, which was explained mainly by the accelerated intersystem crossing[12] and internal conversion[13] based on the exciton coupling theory and conformational dynamics.

O'Keefe et al.[14] reported that Zn^{II} porphyrin dimers possessing butadiyne bridges between the porphyrins, which allow π-electronic conjugation extending to the two porphyrin rings, exhibit an apparent photoinduced absorption band at the near-infrared (NIR) region arising from a triplet−triplet transition. They also reported that the intersystem crossing rate from the lowest singlet state (S_1) to the lowest triplet state (T_1) is of the order of tens of picoseconds. Compared to Zn^{II} porphyrin monomer with the intersystem crossing time of the order of a few nanoseconds, the above intersystem crossing rate is exceptionally fast. Meanwhile, Chachivilis et al.[15] reported that the S_1 state of an ethylene bridged porphyrin dimer has an extraordinarily short lifetime of around several picoseconds. Photoisomerization-like conformational relaxation in the S_1 state was proposed to explain such a fast decay of the excited state of the porphyrin chromophores linked by π-conjugated bridges.

Therefore, it is of interest to investigate the energy relaxation dynamics of porphyrin dimers without π-conjugated bridges because they give additional complexity to the interaction between the porphyrin macrocycles. In this respect, our directly meso−meso linked Zn^{II} porphyrin dimers with different dihedral angles between the porphyrin macrocycles (Scheme 1) are of particular interest and amenable to comparative studies on the energy relaxation dynamics by using various time-resolved spectroscopic techniques.

SCHEME 1

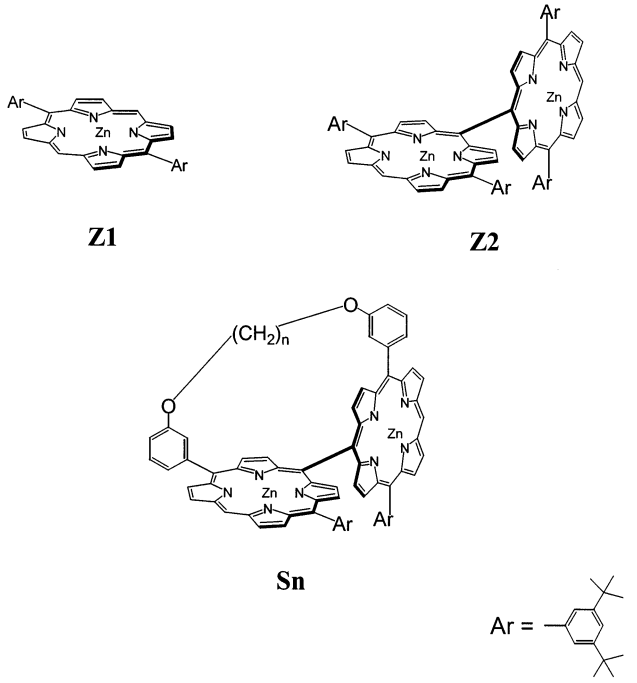

2. Experimental Section

Sample Preparation and Steady-State Measurement. Zn(II) 5,15-bis(3,5-dibutylphenyl)porphyrin (**Z1**) and its meso−meso linked orthogonal dimer (**Z2**) were synthesized through the Ag(I)-promoted meso−meso coupling reaction.[16a] The dihedral angle controlled dimers were synthesized by intramolecular coupling of 1,*n*-dioxymethylene-bridged Zn(II) diporphyrin with a bridge chain of different lengths (We denote the strapped porphyrin dimer as **S*n***, ***n*** = 1, 2, 3, 4, 8, and 10, ***n*** is the number of carbon atoms in the chain) (Scheme 1). The absorption spectra were measured by using a UV/visible spectrophotometer (Varian, Cary-3). The steady-state fluorescence was dispersed by a 20 cm focal length monochromator (Jobin-Yvon, 300 grooves/mm grating) and was detected with an electrically cooled Ge detector (Hamamatsu, M/N B4635). We used two light sources for the steady-state fluorescence studies: a 500 W xenon lamp with a dispersion monochromator and SHG output beam of a CW mode-locked femtosecond Ti:sapphire laser (Coherent, MIRA). Fluorescence excitation spectra were recorded on a scanning SLM-AMINCO 4800 spectrofluorometer, in which we could obtain the corrected spectra by using rhodamine B as a reference quantum counter.

Time-Correlated Single Photon Counting Technique. Picosecond time-resolved fluorescence experiments were carried out by using the time-correlated single photon counting (TCSPC) method.[17] Picosecond excitation pulses were obtained from a homemade cavity-dumped Ti:sapphire laser pumped by a CW Nd:YVO_4 laser (Coherent, Verdi). The second harmonic generation from the cavity-dumped Ti:sapphire laser has ~0.1 ps pulse width and an average power of ca. 1 mW at 400 kHz dumping rating. The emission was collected at 45° with respect to the excitation laser beam by 5- and 25-cm focal length lenses, focused onto a monochromator (Roper Scientific, spectrapro300i), and detected with a microchannel plate photomultiplier tube (Hamamatsu R2809U). The signal was amplified by a wideband amplifier (Philip Scientific), sent to a Quad constant fraction discriminator (Tennelec), a time-to-amplitude converter (Tennelec), a counter (Ortec), and a multichannel analyzer (Tennelec/Nucleus), and stored in a computer.

Femtosecond Transient Absorption Measurements. The dual-beam femtosecond time-resolved transient absorption spectrometer consisted of a self-mode-locked femtosecond Ti:sapphire oscillator (Coherent, MIRA), a Ti:sapphire regenerative amplifier (Clark MXR, CPA-1000) pumped by a Q-switched Nd:YAG laser (Clark MXR, ORC-1000), a pulse stretcher/compressor, OPA (Light Conversion, TOPAS) system, and an optical detection system.[18a] A femtosecond Ti:sapphire oscillator pumped by a CW Nd:YVO_4 laser (Coherent, Verdi) produces a train of ~80 fs mode-locked pulses with an average power of 650 mW at 800 nm. The amplified output beam regenerated by chirped pulse amplification (CPA) had ca. 150 fs pulse width and a power of ca. 1 W at 1 kHz repetition rate, which was divided into two parts by a 1:1 beam splitter. One was color-tuned for the pump beam by the optical parametric generation and amplification (OPG-OPA) technique. The resulting laser pulse had a temporal width of ~150 fs in the UV/vis/IR range. The pump beam was focused to a 1 mm diameter spot and the laser fluence was adjusted to avoid the damage of sample by using a variable neutral-density filter. The other was focused

onto a flowing water cell to generate a white light continuum, which was again split into two parts. The one part of the white light continuum was overlapped with the pump beam at the sample to probe the transient, whereas the other part of the beam was passed through the sample without overlapping the pump beam. The time delay between pump and probe beams was controlled by making the pump beam travel along a variable optical delay. The white light continuum beams after the sample were sent to a 15 cm focal length spectrograph (Acton Research) through each optical fiber and then detected by a dual-channel 512 channel photodiode array (Princeton Instruments). The intensity of the white light continuum of each 512 channel photodiode array was processed to calculate the absorption difference spectrum at the desired time delay between pump and probe pulses.

Femtosecond Fluorescence Upconversion Measurements. The amplified output of the Ti:sapphire laser is divided by a 1:1 beam splitter into two parts. One of them was frequency-doubled by a 0.5 mm LBO crystal to produce the excitation pulses at 400 nm. The excitation beam was loosely focused onto the sample with a spot size of ~1 mm by a concave mirror. The luminescence was collected and focused onto a 1 mm BBO crystal by two identical parabolic mirrors ($f = 70$ mm, $d = 50$ mm). The other part of fundamental laser beam was focused onto the BBO crystal with a spatial overlap with the focused emission spot. The time-delay between pump and gate pulses was controlled with a computer-driven optical delay line. The upconverted UV light was focused onto the entrance slit of a monochromator (Jovin-Yvon, HR320). The scattered light was filtered out with a combination of pinhole and appropriate color filters. The instrumental response was estimated to be ~250 fs from the cross-correlation function between the pump and gate beams.[18a] The output current from a photomultiplier tube (Hamamatsu) was amplified with a fast preamplifier, and then the output voltage was fed into a Boxcar averager (SR250). The resultant signal modulated by a chopper was phase-sensitively measured by a lock-in-amplifier (EG&G) and then fed into a personal computer for further data processing. Much care was taken to avoid a possible saturation of photomultiplier tube due to the short duration of upconverted UV light even though its average power is very low.

3. Results

Figure 1 shows the absorption spectra of **Z1**, **Z2**, and **S*n*** in toluene, indicating that the spectra of **Z2** and **S*n*** are more complicated than that of **Z1**. In the case of **Z2**, the interactions between the two transition dipoles along a longer molecular axis lead to a large splitting of the B-band, whereas a little red shift was observed in the Q-band.[18] In addition to the band splitting/shift, the absorption bands were more broadened compared with **Z1** and no blue-shifted absorption band was found in **Z2**. These spectral changes can be explained well by the exciton coupling theory,[11] because only transition dipoles along the longer molecular axis interact with each other, whereas the perpendicular ones do not interact due to their orthogonal arrangement.[18]

The dihedral angle between the two porphyrin macrocycles in **S*n*** decreases by shortening a strap chain (Scheme 1), which is followed by structural distortions and drastic absorption spectral changes. In going from **S10** to **S1**, the absorption spectra exhibit systematic changes both in the B- and Q-band regions, whereas **S10** exhibits split Soret bands at 414 and 447 nm similar to those of **Z2** except for a slight broadening. The symmetry lowering from D_{2d} to D_2 lifts the degeneracy of excited states

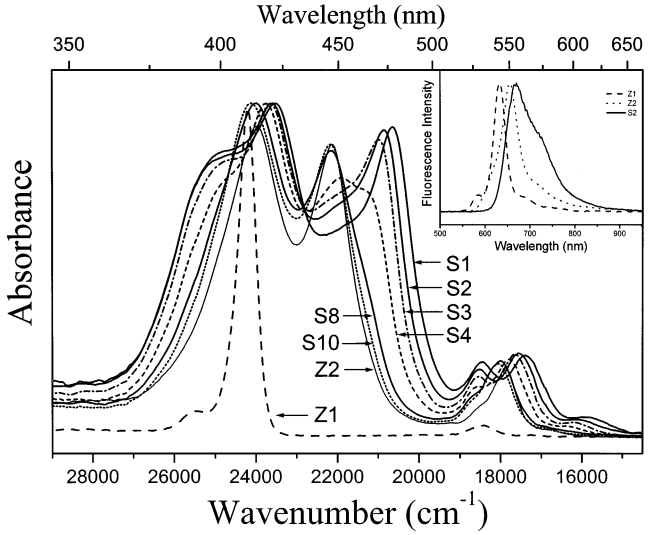

Figure 1. Absorption spectra of **Z1**, **Z2**, and **S*n*** in toluene. The inset shows the fluorescence spectra of **Z1**, **Z2**, and **S2** in toluene after photoexcitation at 400 nm.

in **S*n***, which gives rise to the splitting of the B_y-B_z pair following the exciton coupling scheme, where B_y and B_z denote two perpendicular components of transition dipoles along the intermolecular axis. The intensities of the split Soret bands around 415 and 450 nm decrease and the absorption bands around 400 and >460 nm are intensified, particularly in **S3**, **S2**, and **S1**. In **S2**, the monomeric band at 412 nm is split into two bands at 397 and 424 nm by interactions between the two degenerate transition dipoles perpendicular to the intermolecular axis. The split band from the monomeric B-band indicates that there exist interactions between the parallel transition dipole moments such as the case of H-aggregates.[11] The strong interactions along the intermolecular axis give rise to the absorption band at 478 nm, whereas the higher energy split band is not allowed due to out-of-phase interference of transition dipoles. In the absorption spectrum of the most planar **S1**, three distinct bands are observed at 395, 425, and 483 nm in the Soret band region. Along with these changes, the Q-bands display systematic changes including a change from a prominent Q(1,0) band at 552 nm and a weak Q(0,0) band at 589 nm in **S10** to distinct Q(2,0) and Q(1,0) bands at 540 and 572 nm, and a weak Q(0,0) band at 625 nm in **S1**.

In **S*n***, the exciton coupling framework suggests that the dipole-allowed $B_x + B_x$ states should appear at the same position for all the strapped diporphyrins, because the Coulombic interaction between $B_x + B_x$ should be zero, being independent of the dihedral angle. However, the exciton split B-band of **S1** is further red-shifted from 450 to 483 nm. It has also been calculated by INDO/S-SCI that the spectral change is caused essentially by the dihedral angle, where the ring distortion enhances the red shift of the split B-band.[16c] In addition, the cumulenic resonance interaction should be considered to be responsible for the enhanced red shift of the split B-band.

The structures of **S*n*** estimated by MM2 calculations have indicated that the porphyrin rings in **S10** and **S8** are almost flat with negligible mean plane deviations and arranged roughly in a perpendicular manner with the dihedral angles along the meso−meso linkage of 94° and 89°, respectively. For **S*n*** with shorter straps, the dihedral angles have been calculated as follows: 79° (**S6**), 75° (**S5**), 70° (**S4**), 47° (**S3**), 41° (**S2**), and 36° (**S1**). The X-ray data of Cu(II) complexes of **Z2**, **S2**, **S4**, and **S8** analogues have also provided very useful structural information on their corresponding Zn^{II} porphyrin dimers.[16c]

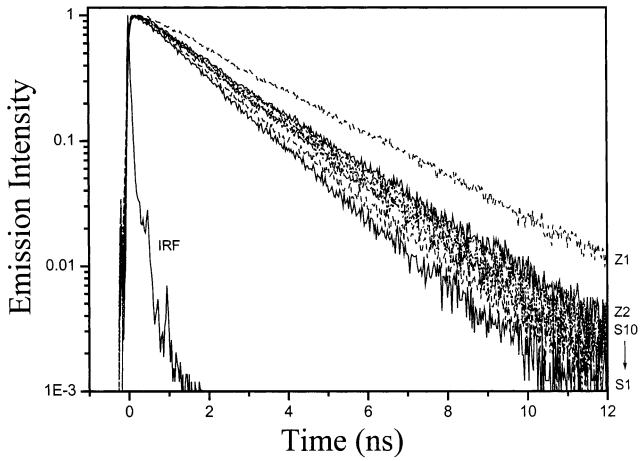

Figure 2. Fluorescence decay profiles of strapped porphyrin dimers (**S*n***) in toluene observed at 630 nm after photoexcitation at 400 nm.

It reveals that **Z2**(Cu) is composed of two quite planar porphyrin rings (the mean plane deviation of porphyrin ring; $\varphi = 0.05$ Å) linked via orthogonal conformation. On the other hand, a single structure of **S8**(Cu) exhibiting two ruffled porphyrin rings ($\varphi = 0.33$ and 0.35 Å) connected by the meso−meso bond length of $\chi = 1.50$ Å with dihedral angles ($\theta_1 = 64.9°$ and $\theta_2 = 80°$, where θ_1 and θ_2 are the dihedral angles between porphyrins at strapped and unstrapped sides, respectively) was observed. In **S2**(Cu) and **S4**(Cu), two different conformers (A and B) packed in a pairwise manner were observed. In the crystal of **S2**(Cu), the A conformer exhibits $\varphi = 0.46$ and 1.30 Å, $\theta_1 = 50.6°$, $\theta_2 = 59.4°$, and $\chi = 1.52$ Å and the B conformer exhibits $\varphi = 0.15$ and 1.64 Å, $\theta_1 = 50.3°$, $\theta_2 = 55.0°$, and $\chi = 1.48$ Å. Similarly, in **S4**(Cu), the A conformer exhibits $\varphi = 0.65$ and 0.72 Å, $\theta_1 = 60.8°$, $\theta_2 = 67.5°$, and $\chi = 1.53$ Å and the B conformer exhibits $\varphi = 0.61$ and 0.70 Å, $\theta_1 = 53.2°$, $\theta_2 = 58.8°$, and $\chi = 1.47$ Å. We note that the A and B conformers have nearly the same mean plane deviations but differ largely in the meso−meso bond length, which is longer in the A conformer and shorter in the B conformer.

The inset of Figure 1 shows the steady-state fluorescence spectrum of **S2** in toluene as well as those of **Z1** and **Z2**. It is worth noting that **S2** exhibits a broad fluorescence spectrum extended to the NIR region with a large red shift (∼1000 cm^{-1}), whereas the spectral bandwidth of **Z2** is similar to that of **Z1** with a little red shift (∼500 cm^{-1}). The fluorescence spectrum of **S2** also reveals a shoulder at 725 nm in addition to the main band at 670 nm.

Figure 2 represents the fluorescence decay profiles of **S*n***, which show similar temporal profiles with single-exponential decay, indicating that the lifetimes of the lowest excited singlet states of **S*n*** are quite similar despite their structural distortions such as mean plane deviations and existence of two conformers. However, although the time constant of **S10** (1.96 ns) is comparable to the fluorescence lifetime (1.98 ns) of **Z2**, the time constant gradually decreases, i.e., 1.84, 1.82, 1.77, 1.65, and 1.53 ns for **S8**, **S4**, **S3**, **S2**, and **S1**, respectively. Judging from X-ray data and MM2 calculations of **S*n***, we can find a trend that the mean plane deviations become gradually severe in going from **S10** to **S1**. In this regard, a systematic decrease in the overall fluorescence lifetimes suggests that the porphyrin ring distortions of **S*n*** have a good correlation with the overall fluorescence lifetimes as compared with **Z2** having planar porphyrin rings. However, it seems that the existence of two conformers in **S1**−**S4** does not influence much the overall fluorescence decay despite different interporphyrin distances.

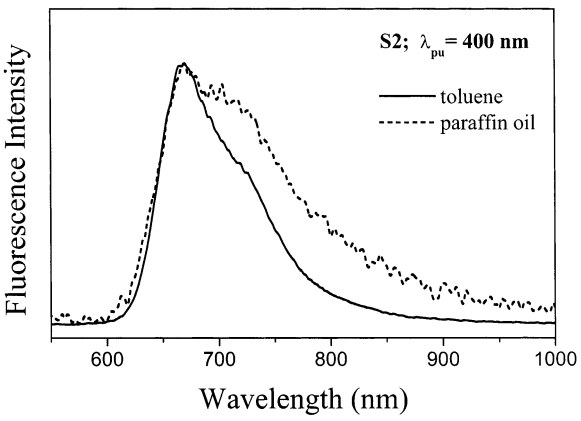

Figure 3. Fluorescence spectra of **S2** in toluene and paraffin oil after photoexcitation at 400 nm. The relative fluorescence intensity at around 725 nm becomes more enhanced in paraffin oil.

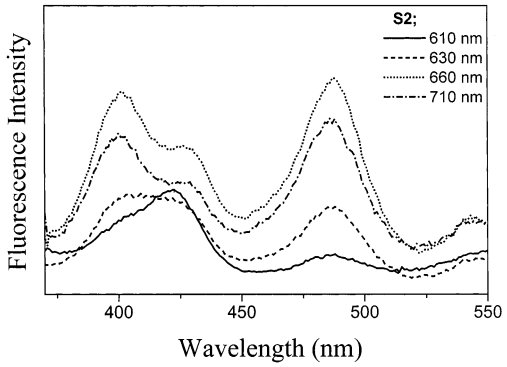

Figure 4. Fluorescence excitation spectra of **S2** in toluene. The fluorescence was monitored at 610, 630, 660, and 710 nm.

In **S*n***, charge-transfer states are accidentally located in the energy region spanned by the split Soret bands. However, no charge-transfer or charge-resonance transitions but only Q-bands exist near the S_1 region, which explains why the overall lowest excited-state decay of strapped diporphyrins is not affected much by a change in the dihedral angle as well as the interporphyrin distance. Therefore, although there is a remarkable change in the absorption spectra of **S*n*** due to the change in the dihedral angle and the concomitant mean plane deviations, the fluorescence decay dynamics of **S*n*** are not so significantly perturbed compared with those of **Z2**.

To explore the conformational dynamics, if any, possibly occurring in much faster time scale, **S2** is suggested to be a representative candidate having a small dihedral angle with two conformers, because **S1** becomes disintegrated slowly under prolonged laser light illumination and the conformational effect induced by the reduced dihedral angle was observed to be not so large in **S4**. Figure 3 shows that the relative fluorescence intensity of **S2** at around 725 nm increases in a viscous paraffin oil medium in comparison with the toluene solution, indicating that the fluorescence spectrum of **S2** originates from two different species. Figure 4 shows the fluorescence excitation spectra of **S2** in toluene monitored at 610, 630, 660, and 710 nm, which reveal that none of them match well with the absorption spectra.

The split energy between the bands at 397 and 424 nm and the relative intensity of the band at 478 nm increases, as the probe wavelength becomes longer (Figure 4). The two isomers are expected to have different photophysical properties, because the relative intensity between the split bands at 397 and 424 nm is expected to have a close relationship with the conformers

TABLE 1: Fluorescence Lifetimes and Relative Amplitude Ratios of S2 as a Function of Probe Wavelength in Toluene and Paraffin Oil at Room Temperature

		amplitude (%)	
probe wavelength (nm)	lifetime (ns)	toluene	paraffin oil
580	0.015[a] (τ_1)	72	48
	1.65 (τ_2)	28	52
610	0.015 (τ_1)	32	10
	1.65 (τ_2)	66	90

[a] τ_1 was based on the lifetime obtained from fluorescence upconversion experiment.

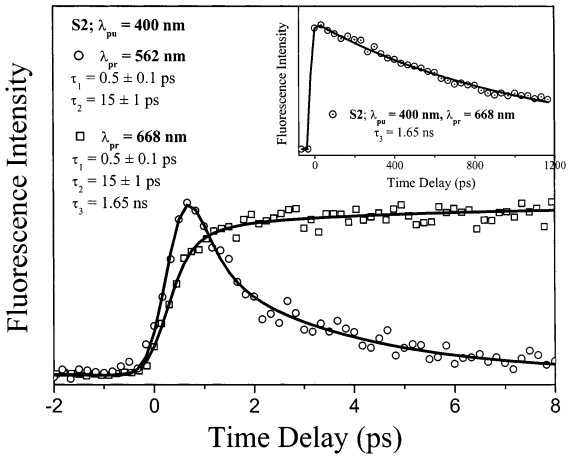

Figure 5. Fluorescence temporal profiles of **S2** at 562 and 668 nm after photoexcitation at 400 nm, which were obtained by the fluorescence upconversion technique. The inset shows the fluorescence temporal profile at 668 nm with the time constant of 1.65 ns in a longer time window after photoexcitation at 400 nm.

having different interporphyrinic distances between the two porphyrin macrocycles; i.e., the B conformer with a shorter interporphyrinic distance is expected to have stronger and more complicated intermolecular interactions than the A conformer. The fluorescence excitation spectra suggest that the A conformer is responsible for the fluorescence at short wavelengths less than ca. 660 nm, whereas the B conformer corresponds to a rather large Stokes-shifted fluorescence at around 720 nm. As another evidence, the relative fluorescence intensity at around 720 nm is enhanced in paraffin oil (Figure 3). These results suggest that there exist at least two emissive isomers having different photophysical properties in **S2**.

The fluorescence decay dynamics of **S2** in toluene and paraffin oil were observed at different probe wavelengths by the TCSPC technique and summarized in Table 1. To investigate the relaxation dynamics of **S2** occurring in the faster time domain, we carried out femtosecond fluorescence upconversion measurements. Figure 5 shows the temporal profiles at the two different probe wavelengths of 562 and 668 nm. The global deconvolution at 562 nm gives the two time constants of ca. 0.5 and 15 ps as decay and rise components, respectively, whereas the two time constants of ca. 0.5 and 15 ps are observed at 668 nm as rise components. In the inset, the time constant of 1.65 ns is also found in a much slower time window at 668 nm.

Figure 6 displays the transient absorption spectra of **Z1**, **S2**, and **Z2** in toluene upon photoexcitation at 400 nm at various time delays. The overall transient absorption spectra of **Z2** are similar to those of **Z1** in the visible/NIR region except its bleaching signal due to the ground-state absorption (Figure 6 and refer to Figure 1). In the NIR region from 700 to 1000 nm, no typical spectral structures have been observed for both **Z1**

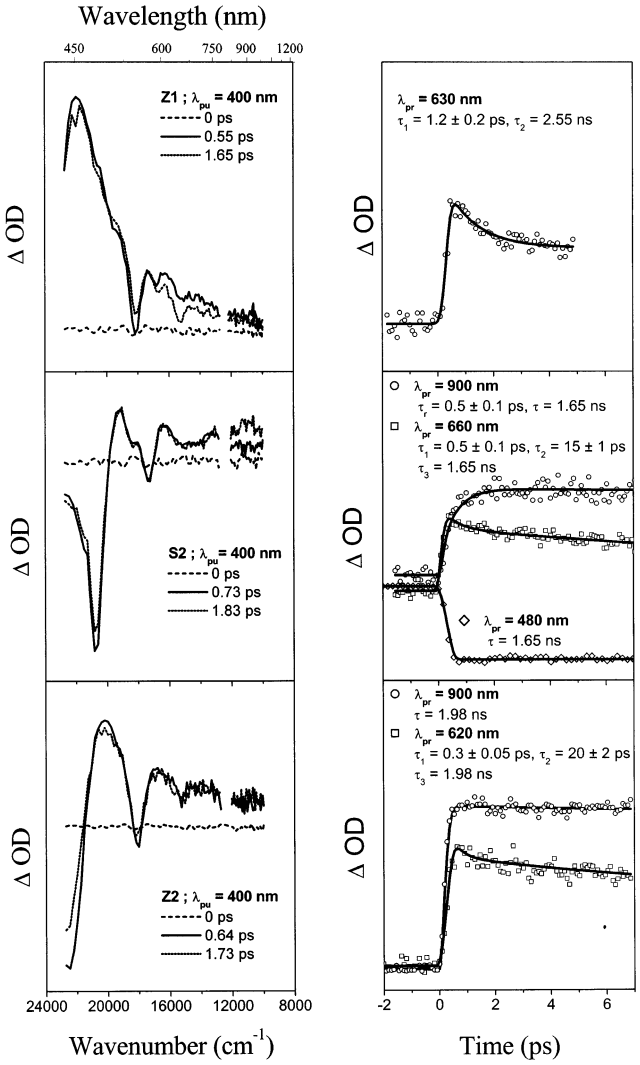

Figure 6. Transient absorption spectra of **Z1** (top), **S2** (middle), and **Z2** (bottom) at three time delays after photoexcitation at 400 nm (left). The transient absorption temporal profiles and fitting results were shown (right).

and **Z2** within a delay time of a few hundred picoseconds. After a long delay time of nanoseconds, however, a pronounced photoinduced absorption band appears at around 800 nm, of which spectral features as well as its dynamics have been well-known to be characteristic of porphyrin triplet−triplet absorption.[19]

Comparison of the stimulated emission band of **S2** with that of **Z2** reveals a noticeable effect of mean plane deviations. **S2** exhibits a broad band structure of the stimulated emission at around 650 nm, of which the bandwidth is about 4 times broader than those of **Z1** and **Z2**. This spectral broadening of the stimulated emission of **S2** in comparison with **Z2** is consistent with the steady-state fluorescence spectra shown in the inset of Figure 1. The decay profiles of **S2** were observed at 480, 660, and 900 nm after photoexcitation at 400 nm, which correspond to the ground-state bleaching, stimulated emission, and photoinduced absorption, respectively (the right side column of Figure 5). The stimulated emission decays with the two different time constants of 0.5 and 15 ps, which are similar to those observed in the fluorescence upconversion experiment (Figure 5). A rise component was also observed with the time constant of 0.5 ps at 900 nm, where a typical pure photoinduced absorption band appears. However, the time constants of 0.5 and 15 ps were hardly observed at 480 nm, in contrast with the cases of the spontaneous emission (Figure 5), stimulated emission at 660

nm and photoinduced absorption at 900 nm (Figure 6). According to the fluorescence excitation spectra, the B conformer rather than the A conformer was photoexcited predominantly by 400 nm optical pulses, though it cannot be ruled out that a little portion of the A conformers were also excited due to the spectral conjecture of the two conformers. However, we could not observe any significant changes in the energy relaxation dynamics when the pumping wavelength decreased from 400 to 395 nm.

4. Discussion

The photophysical properties of the isomers in ethylene-bridged Zn^{II} porphyrin dimer (*trans*-1,2-bis(meso-octaethylporphyrinyl)ethene) were reported by Chachisvilis et al.[15] The exciton split bands of these dimeric conformers appear in the range of 450−900 nm according to their structures. The U conformer is responsible for not only the additional absorption in the 480−500 and 600−850 nm regions but also the unusual fluorescence in the NIR region (750−1100 nm). Its geometrical structure was also proposed to have a common conjugation between the π-orbitals of the porphyrin rings and the ethylene bond. Therefore the cumulenic resonance as well as excitonic interaction explains the intermolecular interactions of the porphyrin dimers linked by π-conjugated bridges. On the contrary, **S2** has relatively weaker interactions between the porphyrin moieties, showing that the absorption and fluorescence bands are less red shifted. Then, why does **S2** have the weaker interactions despite the shorter interporphyrinic distance? First, it must be pointed out that the ethylene bridge could extend the π-conjugation length and hence lowers the energy of the lowest excited state. The time-resolved microwave conductivity experiment indicated that the electronic interaction between the porphyrin units increases, as the length of the intervening bridge increases due to the change of polarizability volume in the series of the ethylene bridged dimers.[20] In other words, the interchromophoric coupling depends on the specific nature of the bridge and thus a simple dependence on the distance may be no longer valid. Second, the steric hindrance between the closest hydrogen atoms makes it difficult to have a coplanar geometry without a sufficient elongation of meso−meso bond, which results in much smaller cumulenic resonance interaction in **S2** than that in the ethylene bridged porphyrin dimer. On the other hand, the rather strong blue-shifted absorption band at 397 nm relative to the monomeric B-band led us to suppose that the contribution of the Coulombic interaction between the two parallel transition dipole moments of each monomer unit is more appreciable in **S2** due to the shorter interporphyrinic distance.

The two time constants of 0.5 and 15 ps were found in the stimulated emission decay profiles of **S2** observed at 660 nm. However, such time constants of 0.5 and 15 ps were not observed in the ground-state bleaching recovery at 480 nm, indicating that these time constants do not result from the direct electronic transition to the ground state but the excited state in **S2** (Figure 6). The NIR photoinduced absorption at 900 nm grows with the time constant of 0.5 ps and decays with the time constant of 1.65 ns. The triplet-state absorption of **S2** might be considered as one of possible candidates for the NIR photoinduced absorption, because it has been well-known that both the triplet−triplet and free cationic absorption bands of porphyrin moieties usually appear in the NIR region and the formation time of triplet states in the dimer is accelerated with respect to the monomer.[12] The formation time constant of 0.5 ps, however, is still too fast to be responsible for the intersystem crossing and ionization processes for the energy relaxation mechanism because of the strong fluorescence of **S2** (quantum yield = 0.036 for **S2** and 0.025 for **Z2** in benzene at room temperature). In addition, the time constant of 1.65 ns was revealed to originate from the direct electronic transition from the excited singlet states to the ground state by the transient absorption measurement. Therefore, it is relevant to attribute the observed NIR band to the photoinduced absorption between the excited singlet states rather than the triplet−triplet absorption or the ionization process of **S2**. Following fast energy relaxation dynamics with the time constant of 0.5 ps, the lowest excited states relax slowly with the time constant of 1.65 ns. The 0.5 ps time constant of **S2** is a little slower than that of **Z2** (0.3 ps), which is consistent with a trend that the internal conversion to the lowest excited-state becomes slower as the exciton split Soret band is more red shifted, because the energy difference between the monomeric Soret band and the split Soret band increases.[18b]

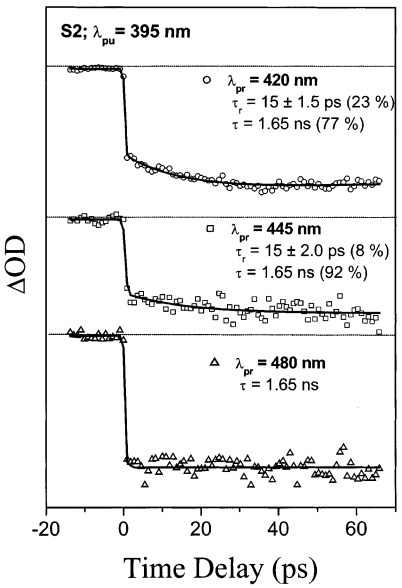

Figure 7. Transient absorption temporal profiles of **S2** at 420, 445, and 480 nm after photoexcitation at 395 nm. A 15 ps component becomes pronounced as the probe wavelength is decreased.

On the other hand, following fast energy relaxation dynamics with the time constant of 0.5 ps, the 15 ps component was also observed in the fluorescence upconversion and stimulated emission decay profiles. Such picosecond dynamics have been observed in various porphyrin systems and explained mainly by the following two arguments: (1) Excess vibrational energy in closed-shell metalloporphyrin monomers is dissipated with a spectral evolution on a 10−20 ps time scale, which is called the vibrational cooling process.[21,22] (2) A lot of cases with a similar time scale are described by invoking the conformational dynamics in the excited states. The unimolecular reactions with such a time scale are related to large structural changes such as the photoisomerization reaction of *trans*-stilbene. The careful inspection shows that the component of a time constant of 15 ps increases in the ground-state bleaching signals, as the probe wavelength decreases from 480 to 420 nm after photoexcitation at 395 nm (Figure 7), which is generally opposite to the vibrational cooling process.[21,22] The photoinduced absorption signal was observed to have a broad spectral feature in this probe region (Figure 6), indicating that the dynamics in the excited states can be mixed with the ground-state bleaching signal. In addition, the component of a time constant of 15 ps in the ground-state bleaching signals at the same probe wavelength, i.e., 420, 445, and 480 nm, were reduced slightly when the pump wavelength was changed from 395 to 400 nm. Therefore we

suggest that the time constant of 15 ps originates from the decay dynamics of the photoinduced absorption, which leads to the conclusion that the conformational dynamics is the most probable arguments.

We note that the conformational dynamics of **S2** (∼15 ps) is a little faster than that of **Z2** (∼20 ps). The existence of two conformers in **S2** is largely responsible for the fast conformational dynamics, whereas it is also suggested that the activation barrier for the conformational dynamics in **S2** is lower on the reaction coordinate.[18a] After Soret band photoexcitation, **Z2** in the excited state in the Franck−Condon region proceeds to reach an equilibrium position on the excited potential energy surface, where the probable reaction coordinate could be ascribed to be the dihedral angle between the porphyrin macrocycles. Unfortunately, however, it is difficult to assign the reaction coordinate in **S2** clearly due to the expectedly complicate structural changes.

5. Conclusions

The photophysical properties of various Zn^{II} porphyrin dimers regarding the structure−property relationship were reported on the basis of the steady-state and time-resolved spectroscopic measurements. The fluorescence decay measurements of the strapped porphyrins dimers, **S*n***, show good correlations between the fluorescence lifetimes and the porphyrins ring deviations. The existence of the two conformers in **S1**−**S4** does not affect much the overall fluorescence decay dynamics. On the other hand, the fluorescence excitation spectra of **S2** at various probe wavelengths reveal that there exist at least two different conformers as confirmed by X-ray data, and their excited configuration changes are dependent on the solvent viscosity. A careful comparative femtosecond spectroscopic investigation between **Z2** and **S2** reveals that there exists conformational dynamics with a time constant of ∼15 ps after a rapid population (∼0.5 ps) of the lowest excited state of **S2**. Finally, the electronic interactions between the porphyrins of the dimers, which are mainly determined by the dihedral angle, interporphyrin distance, and types of linkers, if any, play an important role in their energy relaxation dynamics.

Acknowledgment. The work at Yonsei University has been financially supported by the National Creative Research Initiatives Program of the Ministry of Science & Technology of Korea. The work at Kyoto was supported by CREST (Core Research for Evolutional Science and Technology) of the Japan Science and Technology Corporation (JST).

Supporting Information Available: Structures and structural parameters of free-base diporphyrins estimated by MM2 calculations and transient absorption temporal profiles of **S2**. This material is available free of charge via the Internet at http://pubs.acs.org.

References and Notes

(1) (a) *Photosynthetic Light-Harvesting Systems*; Scheer, H., Schneider, S., Eds.; de Gruyter: Berlin, 1988. (b) Pearlstein, R. M. In *Chlorophylls*; Scheer, H., Ed.; CRC Press: Boca Raton, FL, 1991; p 1047. (c) Sundström, V.; van Grondell, R. In *Chlorophylls*; Scheer, H., Ed.; CRC Press: Boca Raton, FL, 1991; p 1097. (d) van Grondell, R.; Dekker: J. P.; Gillbro, T.; Sundström, V. *Biochim. Biophys. Acta* **1994**, *1187*, p 1. (e) Sundström, V.; Pullerits, T.; van Grondelle, R. *J. Phys. Chem. B* **1999**, *103*, 2327.

(2) Fleming, G. R.; van Grondelle, R. *Phys. Today* **1994**, 48.

(3) (a) Wagner, R. W.; Lindsey, J. S.; Seth, J.; Palaniappan, V.; Bocian, D. F. *J. Am. Chem. Soc.* **1996**, *118*, 3996. (b) Wagner, R. W.; Lindsey, J. S. *J. Am. Chem. Soc.* **1994**, *116*, 9759. (c) Martin, R. E.; Diederich, F. *Angew. Chem., Int. Ed. Engl.* **1999**, *38*, 1350.

(4) (a) Lin, V. S.-Y.; DiMagno, S. G.; Therien, M. J. *Science* **1994**, *264*, 1105. (b) Lin, V. S.-Y.; Therien, M. J. *Chem. Eur. J.* **1995**, *1*, 645.

(5) (a) Ponomarev, G. V.; Borovkov, V.; Sugiura, K.; Sakata, Y.; Shul'ga, A. *Tetrahedron Lett.* **1993**, *34*, 2153. (b) Senge, M. O.; Gerzevske, K.; Vicente, M. G. H.; Forsyth, T.; Smith, K. M. *Angew. Chem., Int. Ed. Engl.* **1993**, *32*, 750. (c) Ponomarev, G. V.; Borovkov, V.; Shul'ga, A.; Sakata, Y. *J. Chem. Soc., Chem. Commun.* **1994**, *32*, 750. (d) Senge, M. O.; Vicente, M. G. H.; Gerzevske, K.; Forsyth, T.; Smith, K. M. *Inorg. Chem.* **1994**, *33*, 5625. (e) Higuchi, H.; Takeuchi, M.; Ojima, J. *Chem. Lett.* **1996**, 593.

(6) (a) Arnold, D. P.; Nitschinsk, L. J. *Tetrahedron* **1992**, *48*, 8781. (b) Arnold, D. P.; Nitschinsk, L. J. *Tetrahedron Lett.* **1993**, *34*, 693.

(7) (a) Vicente, M. G. H.; Smith, K. M. *J. Org. Chem.* **1991**, *56*, 4407. (b) Vicente, M. G. H.; Jaquinod, L.; Smith, K. M. *Chem. Commun.* **1999**, 1771.

(8) (a) Burrell, A. K.; Officer, D. L.; Reid, D. C. W. *Angew. Chem., Int. Ed. Engl.* **1995**, *34*, 900. (b) Burrell, A. K.; Officer, D. L. *Synlett.* **1998**, 1297.

(9) (a) Osuka, A.; Liu, B.-L.; Maruyama, K. *Chem. Lett.* **1993**, 949. (b) Osuka, A.; Maruyama, K.; Mataga, N.; Asahi, T.; Yamazaki, I.; Tamai, N. *J. Am. Chem. Soc.* **1990**, *112*, 4958. (c) Osuka, A.; Nakajima, S.; Maruyama, K.; Mataga, N.; Asahi, T.; Yamazaki, I.; Nishimura, Y.; Ohno, T.; Nozaki, K. *J. Am. Chem. Soc.* **1993**, *115*, 4577. (d) Osuka, A.; Maruyama, K. *J. Am. Chem. Soc.* **1988**, *110*, 4454. (e) Osuka, A.; Maruyama, K.; Yamazaki, I.; Tamai, N. *J. Chem. Soc., Chem. Commun.* **1988**, 1243. (f) Osuka, A.; Maruyama, K.; Yamazaki, I.; Tamai, N. *Chem. Phys. Lett.* **1990**, *165*, 392.

(10) (a) Yang, S. I.; Lammi, R. K.; Seth, J.; Riggs, J. A.; Arai, T.; Kim, D.; Bocian, D. F.; Holten, D.; Lindsey, J. S. *J. Phys. Chem. B* **1998**, *102*, 9426. (b) Strachan, J. P.; Gentemann, S.; Seth, J.; Kalsbeck, W. A.; Lindsey, J. S.; Holten, D.; Bocian, D. F. *J. Am. Chem. Soc.* **1997**, *119*, 11191. (c) Yang, S. I.; Seth, J.; Balasubramanian, T.; Kim, D.; Lindsey, J. S.; Holten, D.; Bocian, D. F. *J. Am. Chem. Soc.* **1999**, *121*, 4008.

(11) Kasha, M.; Rawls, H. R.; El-Bayoumi, M. A. *Pure Appl. Chem.* **1965**, *11*, 371.

(12) McRae, E. G.; Kasha, M. *J. Chem. Phys.* **1958**, *28*, 721.

(13) Sundström, V.; Tomas, G. *J. Chem. Phys.* **1985**, *83*, 2733.

(14) O'Keefe, G. E.; Denton, G. J.; Harvey, E. J.; Philips, R. T.; Friend, R. H.; Anderson, H. L. *J. Chem. Phys.* **1996**, *104*, 805.

(15) (a) Chachisvilis, M.; Chirvony, V. S.; Shulga, A. M.; Källebring, B.; Larsson, S.; Sunström, V. *J. Phys. Chem.* **1996**, *100*, 13857. (b) Chachisvilis, M.; Chirvony, V. S.; Shulga, A. M.; Källebring, B.; Larsson, S.; Sunström, V. *J. Phys. Chem.* **1996**, *100*, 13867.

(16) (a) Osuka, A.; Shimizu, H. *Angew. Chem., Int. Ed. Engl.* **1997**, *36*, 135. (b) Yoshida, N.; Osuka, A. *Org. Lett.* **2000**, *2*, 2963. (c) Yoshida, N.; Jeong, D. H.; Cho, H. S.; Kim, D.; Matsuzaki, Y.; Tanaka, K.; Osuka, A. *Chem. Eur. J.* **2003**, *9*, 58.

(17) Lee, M.; Kim, D. *J. Opt. Soc. Korea* **1990**, *1*, 52.

(18) (a) Cho, H. S.; Song, N. W.; Kim, Y. H.; Jeoung, S. C.; Hahn, S.; Kim, D.; Kim, S. K.; Yoshida, N.; Osuka, A. *J. Phys. Chem. A* **2000**, *104*, 3287. (b) Kim, Y. H.; Jeong, D. H.; Kim, D.; Jeoung, S. C.; Cho, H. S.; Kim, S. K.; Aratani, N.; Osuka, A. *J. Am. Chem. Soc.* **2001**, *123*, 76. (c) Kim, Y. H.; Cho, H. S.; Kim, D.; Kim, S. K.; Yoshida, N.; Osuka, A. *Synth. Met.* **2001**, *117*, 183. (d) Song, N. W.; Cho, H. S.; Yoon, M.-C. Jeoung, S. C.; Kim, D.; Yoshida, N.; Osuka, A. *Bull. Chem. Soc. Jpn.* **2002**, *75*, 1023. (e) Aratani, N.; Osuka, A.; Cho, H. S.; Kim, D. *J. Photochem. Photobiol. C: Photochem. Rev.* **2002**, *3*, 25.

(19) (a) Rodrigues, J.; Kirmaier, C.; Holten, D. *J. Am. Chem. Soc.* **1989**, *111*, 6500. (b) Song, N. W.; Cho, H. S.; Yoon, M.-C.; Aratani, N.; Osuka, A.; Kim D. *Bull. Korean Chem. Soc.* **2002**, *23*, 271.

(20) Piet, J. J.; Taylor, P. N.; Anderson, H. L.; Osuka, A.; Warman, J. M. *J. Am. Chem. Soc.* **2000**, *122*, 1749.

(21) Rodriguez, J.; Kirmaier, C.; Holten, D. *J. Chem. Phys.* **1991**, *94*, 6020.

(22) Eom, H. S.; Jeoung, S. C.; Kim, D.; Ha, J.-H.; Kim, Y.-R. *J. Phys. Chem. A* **1997**, *101*, 3661.